SCIENTIFIC PAPER
Published: September 17, 2025
https://doi.org/10.13167/2025.31.6

Assessment of building envelope thermal insulation and indoor air temperature

Azzam Alosaimi[1]✉

[1] *Jazan University, Collage of Engineering and Computer Science, Department of Civil and Architectural Engineering, Al Maarefah Rd, 82817, Alshati, Jazan, Saudi Arabia*

Corresponding author:
Azzam Alosaimi

Received:
November 4, 2024

Revised:
August 19, 2025

Accepted:
September 1, 2025

Published:
September 17, 2025

Citation:
Alosaimi, A. Assessment of building envelope thermal insulation and indoor air temperature. *Advances in Civil and Architectural Engineering,* 2025, 16 (31), pp. 83-110. https://doi.org/10.13167/2025.31.6

ADVANCES IN CIVIL AND ARCHITECTURAL ENGINEERING (ISSN 2975-3848)

Faculty of Civil Engineering and Architecture Osijek
Josip Juraj Strossmayer University of Osijek
Vladimira Preloga 3
31000 Osijek
CROATIA

Abstract:
This study investigated the impact of thermal insulation placement, type and thickness on indoor air temperature (IAT), energy performance and electricity costs for a residential villa in the hot-humid climate of Jazan, Saudi Arabia. A baseline EnergyPlus model, validated against measured data from Riyadh, revealed that without insulation, IAT exceeded American Society of Heating, Refrigerating and Air-Conditioning Engineers (ASHRAE) comfort limits for 93 % of the year. Simulations of five common insulation types, including board, batt, cellular glass, fibreglass and polyurethane, demonstrated that exterior placement consistently outperformed interior installation by reducing heat transfer and infiltration. Polyurethane delivered the highest performance, achieving up to a 40,2 % reduction in annual energy use at 100 mm thickness, with diminishing returns beyond 75-100 mm. A floor-level analysis revealed that upper floors with exposed roofs required thicker insulation to counteract solar gains, whereas lower floors performed optimally with thinner layers in humid conditions. An economic analysis based on Saudi Arabia's residential tariff structure demonstrated lifetime savings exceeding USD 79.760,00 over 20 years for top-performing configurations. The findings underscore the importance of climate- and building-specific insulation strategies to optimise both thermal comfort and long-term economic returns.

Keywords:
EnergyPlus modelling; energy performance; thermal insulation; indoor air temperature; sensitivity analysis

1 Introduction

The global reliance on fossil fuels remains the primary driver of greenhouse gas (GHG) emissions and environmental degradation. Approximately 75 % of GHG emissions originate from the combustion of non-renewable energy sources such as coal, oil, and natural gas, which continue to dominate global energy production despite their finite nature and adverse health impacts [1]. These emissions are associated with approximately 12,1 million premature deaths annually, underscoring the urgency for sustainable energy strategies [2].

As a leading oil producer, Saudi Arabia plays a critical role in the global energy market. The Kingdom holds the second-largest proven petroleum reserves worldwide, contributing approximately 13 % of global crude oil exports and 3 % of the total natural gas supply in 2021 [3]. Its energy mix is dominated by oil (65 %) and natural gas (35 %), which reflects its strong dependence on fossil fuels [4]. Between 2017 and 2022, petroleum-based energy production increased from 17,9 to 20,3 million barrels per day, accounting for approximately 11 % of the global output (see Figure 1) [5]. Concurrently, domestic energy consumption remains high, with Saudi Arabia consuming approximately one-third of its annual production of approximately 3,351 million barrels of oil equivalent [4].

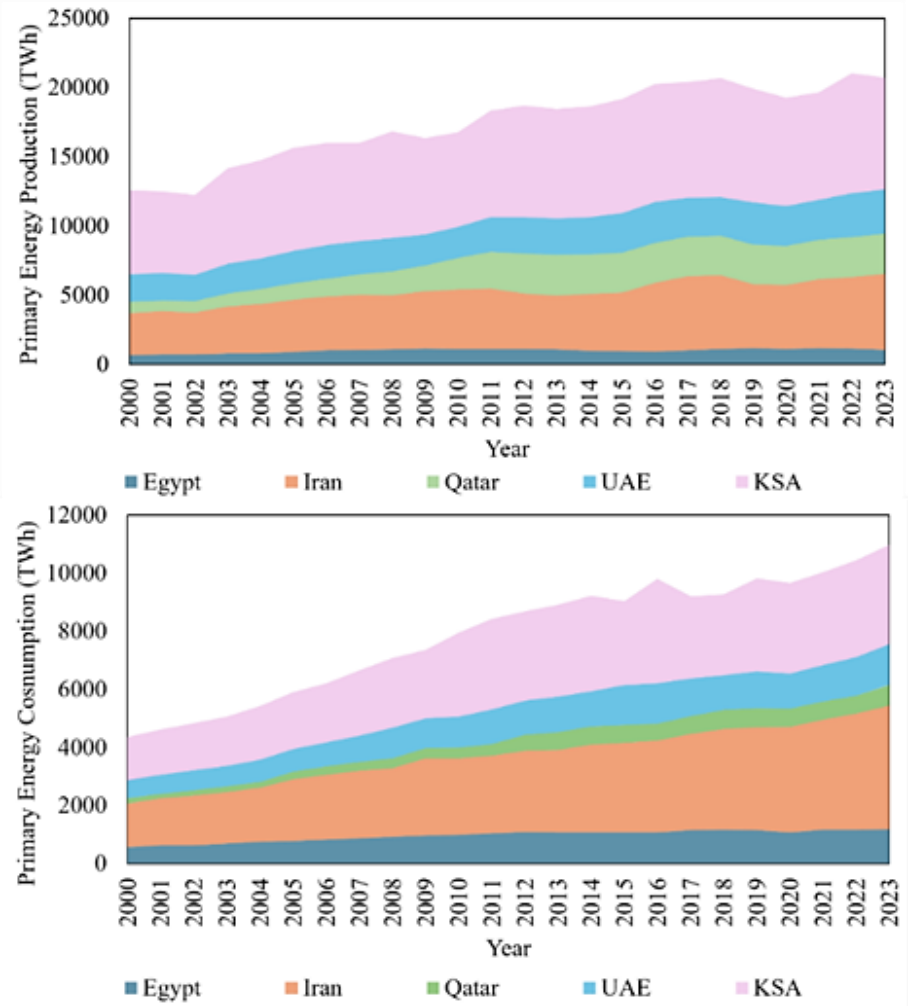

Figure 1. World energy production and consumption for Egypt, Iran, Qatar, the United Arab Emirates (UAE), and the Kingdom of Saudi Arabia (KSA) [1; 3]

Electricity production and consumption have risen sharply since 1990 by more than 80 % and 268 %, reaching 359 and 299 TWh by 2018, respectively [6]. This trend has been driven by rapid population growth and infrastructure expansion. Among the Middle Eastern and North

African (MENA) countries, Saudi Arabia ranks highest in fossil fuel–based electricity generation [3]. Figure 2 compares Saudi Arabia, the largest electricity producer in the Gulf Cooperation Council, with the United Arab Emirates, the second-largest producer. It shows steady growth in generation and consumption from 2010 to 2023, with both countries maintaining their surplus capacity and experiencing a brief decrease in 2020, likely due to COVID-19 [7].

The building sector is a critical focus in this context. It accounts for nearly 75 % of the Kingdom's primary energy consumption, primarily because of the high cooling demand in residential and commercial buildings [4]. According to the Saudi Energy Efficiency Center, energy consumption is concentrated in the industrial (47 %), construction (29 %), and transportation (21 %) sectors, with buildings representing the largest share [8]. Although national-level building energy performance has been extensively reported in the literature, there remains a lack of region-specific studies addressing strategies to reduce building energy demand and carbon emissions in the Jazan region.

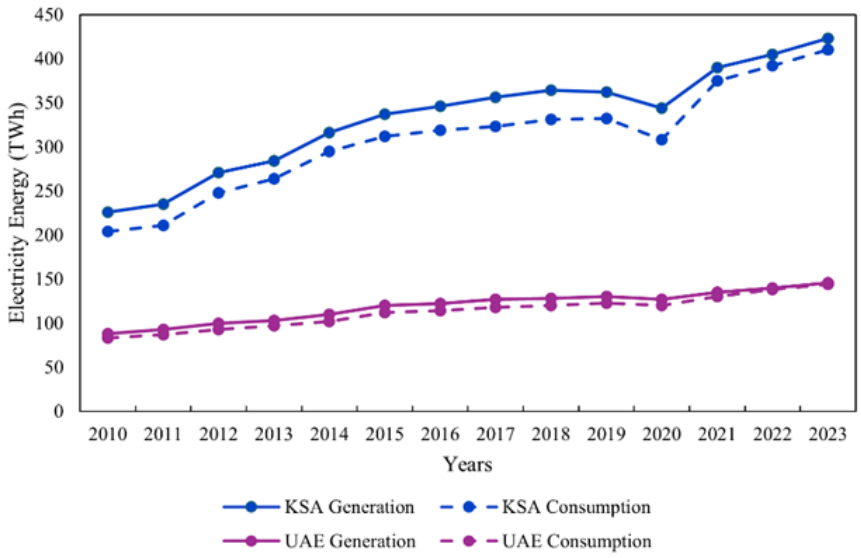

Figure 2. The highest electricity producers and consumers in the Middle East and North Africa area (chart from [7])

2 Literature review

This literature review extensively explores the building energy demands in Saudi Arabia and emphasises the necessity of formulating energy assessments to mitigate energy demands and minimise carbon emissions.

2.1 Building energy optimisation

Research on building energy optimisation in Saudi Arabia can be categorised into early and recent studies. Early studies, published in the late 1980s and early 1990s, focused on the influence of weather variations on building energy performance. The primary objective of these studies was to develop representative datasets for weather variations that could be utilised in future building energy analyses in Saudi Arabia. Initial efforts by different researchers aimed to collect meteorological data from major Saudi cities for the period between 1970 and 1991. These studies released weather characteristics for 20 cities across distinct climatic zones, including air temperature, humidity, and degree-day base temperature [9]. Said, Habib, and Iqbal reported details on outdoor design conditions, degree days, bin data, and weather datasets derived from extensive weather histories spanning 20-30 years. These weather datasets are an invaluable resource for engineers and researchers engaged in the field of

energy conservation in buildings. Furthermore, the significance of weather datasets was articulated specifically for dynamic energy calculations to capture building energy behaviour. However, recent studies have utilised weather data generated by earlier research to investigate building energy performance and to identify the most influential factors influencing energy demand. These recent studies can be classified into experimental and simulation-based approaches [10]. Experimental studies have adopted actual building experiments by controlling building environments and observing changes, whereas simulation studies have focused on constructing energy models that replicate real building energy performances. These models are validated by comparing simulated outputs with electricity bills and used to evaluate various energy efficiency measures [11; 12].

Three techniques have been used to conduct building energy performance assessments: physical measurements in real-life settings, modelling techniques utilising computational tools, and a combination of both approaches. A real-life physical measurement was conducted [13] in Turkey to analyse the energy produced by applying a photovoltaic power plant to a school rooftop. Adopting a modelling technique, Krarti et al. [14] developed a residential building stock model specific to Saudi Arabia to evaluate and reduce energy demands. Huang et al. [15] used a combination of both approaches to evaluate a low-energy ventilation cooling device that addressed the lack of air conditioning during summer. Huang et al. [15] indicated that repurposing discarded plastic bottles for low-energy ventilation cooling devices can serve as an effective strategy for mitigating air pollutants and minimising the negative environmental impact on human health.

Energy analyses of buildings using actual measurements require data on the energy usage, patterns, and efficiency within a constructed space. Actual measurements can be difficult, time-consuming, and expensive [16]; however, energy modelling techniques offer accurate and more flexible building energy assessments. Modelling techniques are favoured over physical building assessments as they offer several advantages. First, they are less expensive and eliminate the need for extensive on-site measurements and evaluations [17]. Secondly, they provide simplicity and flexibility, allowing the exploration of various scenarios and parameters without physical limitations. Finally, they enable an informative decision-making process by offering predictive capabilities for the future energy performance in various scenarios [18].

2.2 Building energy modelling

According to Clarke [19], building energy modelling (BEM) methods are usually developed using mathematical models based on the First Law of Thermodynamics: ‘The Energy Conservation Law contends that energy is not able to be lost during the procedure of changing one type of energy to an alternative and that energy must constantly be saved’. BEM employs two primary approaches: *top-down* and *bottom-up* approaches [17]. The top-down approach utilises aggregated building data on a larger scale, breaking down outputs into specific end uses, whereas the bottom-up approach requires specific data inputs for predetermined buildings, compares them to the total housing stock, and yields more precise results [18]. The bottom-up method requires detailed data inputs, such as building geometry, dimensions, and type. Two distinct types of bottom-up approaches are recognised: statistical and engineering [17]. A comprehensive comparison of the advantages and disadvantages of each approach is presented in Table 1 [7].

BEM can employ steady-state or dynamic methods [20]. Although the steady-state method is simple, it cannot accurately calculate or represent the energy performance of various building systems, highlighting a clear limitation. This limitation hinders the capture of transient effects, such as fluctuating weather conditions or occupant behaviour. Consequently, it operates under the assumption that conditions within a building remain stable over time. In contrast, the dynamic method is better suited to recording energy fluxes and fluctuations as building systems change. This method is implemented effectively using a bottom-up engineering approach. Although the bottom-up engineering method is more complex than the top-down approach, given that it requires a more detailed data input [18], this capability allows for precise

assessments of the indoor air temperatures of individual buildings, enabling a more detailed understanding of the impact of system changes on indoor building conditions.
The BEM is commonly employed to develop an energy model baseline for energy assessment. The baseline serves as a reference tool by enabling assessments of energy performance both before and after changes are made [21]. An energy baseline is usually developed using various energy simulation tools, such as the Integrated Environmental Solution [22], Quest [23], TAS [24], DesignBuilder [25], and EnergyPlus [26], to create a baseline energy model. These simulation tools are typically employed to evaluate a building's energy demands and to determine energy-efficiency scenarios by modifying the building envelope characteristics.
Recent studies conducted in Saudi Arabia have used different simulation tools to perform parametric building energy analyses and implement energy efficiency measures. This approach is advantageous because it offers interesting insights into optimal scenarios prior to decision-making [27; 14; 28]. The BEM technique usually employs sensitivity analysis to evaluate the indoor air temperature (IAT) by testing the impact of different configurations of building thermal envelopes.

Table 1. Comparison of the strengths and weaknesses of each modelling approach [7]

	***Top down* approach**	***Bottom up* (statistical) approach**	***Bottom up* (engineering) approach**
Strengths	Long-term predictions	Occupants' activities	Predicts new technologies
	Macro/socioeconomic impacts	Macro/socioeconomic impact	Bottom-up estimations
	Data input is easy	End-use representation	End-use usages
	Includes trends	Billing data	End-use qualities
Weaknesses	Historical data is required	Historical data are required	Assumptions
	Lacks end-use representations	Multiple correlations	Detailed data inputs
	Coarse analyses	Large samples	Simulation complexity
	No new technologies	Fewer data are provided	Lacks economic factors

2.3 Sensitivity analysis

Sensitivity analysis (SA) examines the changes resulting from fluctuations in the input data. SA is typically performed by quantifying the statistical values of interest to estimate the mean, median, and sample quantiles. These estimates allow technical decision-makers to define key performance metrics. In particular, the examination of uncertainty and sensitivity in modelling techniques allows for better handling of risks by identifying the most significant inputs or risk indicators. Baker et al. [29] identified SA as a crucial statistical tool for risk management. According to Jones [30], SA may assist in the development of climate change mitigation measures by identifying critical uncertainties in forecasting models.
This insight has enabled further investigations, as highlighted by Cullen and Frey [31]. SA plays a role in the ongoing construction and refinement of models, offering a means of verification and validation, as indicated by Kleijnen [32], Fraedrich and Goldberg [33], Philip [34], and Ward [35]. Performing SA for decision-making purposes is both feasible and beneficial, as it aids in understanding the robustness of a model's results. Such understanding allows for additional enquiries [31] and enhances the reliability of model inputs and outputs [31; 36].

2.4 Building a thermal envelope

The term building envelope denotes the physical barrier that separates the interior climate-controlled space from external ambient conditions. Extensive research on building envelopes in Saudi Arabia has predominantly focused on the application of exterior thermal insulation materials to mitigate solar radiation absorption by the envelope [37]. This study spanned diverse regions in Saudi Arabia and strategically assessed the energy efficiency of building

thermal envelopes. Previous investigations have delved into the interplay between the thermal envelopes of buildings and their energy consumption, revealing that 40-45 % of a building's thermal load can be attributed to heat transfer across the envelope [38]. This observation demonstrates the significance of implementing energy-efficient thermal insulation measures to reduce heat transmission through building envelopes in Saudi buildings.

Al-Naimi [39] and Abdelrahman, Said and Ahmad [40] evaluated the energy performance of dwellings in Saudi Arabia to reduce energy demand by identifying energy-efficient thermal envelope materials. They demonstrated that thermal insulation can potentially reduce the energy demand of buildings by approximately 40 %. A decade later, Ahmad [41] analysed a typical housing unit in Dhahran using various types of thermal envelope construction materials. This house was built by the King Fahd University of Petroleum and Minerals to observe the effects of different types of masonry as building materials. The study revealed that constructing a house with gypsum blocks resulted in a significant reduction of 13,2 % in energy consumption compared with the use of heavyweight concrete blocks.

According to Antar and Baig [42] and Antar [43], the thermal envelopes of buildings commonly feature cracks and small openings that allow large quantities of heat to flow into the interior spaces. They formulated parameters for identifying energy-efficient building-envelope components. Antar and Baig [42] numerically investigated conjugate heat transfer across a hollow block by considering conduction heat transfer within the block material and natural convection in the cavity. The results indicated that increasing the number of cavities while maintaining a constant block width substantially increased the resistance of the material, thereby reducing the heat transfer.

Budaiwi [44] explored the impact of different thermal envelopes of different Saudi buildings on the energy demand and revealed that the application of suitable thermal insulation can lead to a reduction in energy consumption. In addition, Al-Sanea et al. [45] focused on the impact of thermal mass quantity and placement within insulated building walls, reporting potential energy savings of 17 % for heating and 35 % for cooling workloads compared with the maximum energy consumption. Moreover, Aldawoud et al. [46] examined double-skin façades (DSFs) and various glazing types and concluded that significant energy savings could be realised. However, the implementation of DSFs is challenging owing to the requirements of additional building areas, construction materials, and higher costs. More recently, Alosaimi [7] assessed the sensitivity of thermal insulation placement on thermal envelopes; however, this assessment was conducted only in the Riyadh region, and no studies have evaluated the thermal insulation of buildings in the Jazan region. The Jazan region, characterised by distinctive features, extreme temperatures and elevated humidity levels, might not demonstrate energy-saving performance comparable to that of other regions. This is primarily due to the unique weather conditions of coastal cities, which include elevated humidity levels. No studies have been conducted in the Jazan region to lower IAT and reduce the energy demand of buildings and greenhouse gas emissions. Therefore, this study aimed to evaluate the internal environmental conditions of a villa located in this region and improve IAT via thermal envelope modifications. To achieve this aim, various thermal insulation types were investigated via SA using the EnergyPlus simulation tool.

3 Methodology

This study adopted an engineering bottom-up dynamic simulation approach implemented using the EnergyPlus simulation tool. This method was chosen because of its ability to account for time-lag effects, thermal damping, and dynamic surface temperature responses. The analysis evaluated the influence of building envelope thermal insulation placement, type, and thickness on IAT, energy performance, and associated electricity costs in a hot-humid climate (see Figure 3).

The assessment was conducted in two stages. In the first stage, the baseline residential building model was simulated in the free-running mode to assess the thermal performance of different insulation configurations under passive conditions, focusing on their impact on the

IAT. In the second stage, the same model was used under active cooling conditions to determine energy demand, and a cost analysis was conducted to quantify the economic implications of each insulation strategy. A one-parameter-at-a-time SA was applied to isolate the effects of each insulation variable, ensuring a clear understanding of the design modifications and performance outcomes.

Owing to the limited availability of empirical building performance data for the Jazan region, the baseline model parameters were adapted from previous studies by Krarti et al. [14] and Alosaimi [7], and more recently, by Alosaimi in 2024 [47]. For validation, the model was initially configured for the Riyadh region, where climatic conditions and benchmark datasets are well documented. The simulation outputs for IAT, cooling loads, and energy use were compared against these benchmarks to verify the accuracy. Once validated, the model was transposed to Jazan's climatic conditions to evaluate the insulation performance in a representative hot-humid environment and achieve the study's primary research objective.

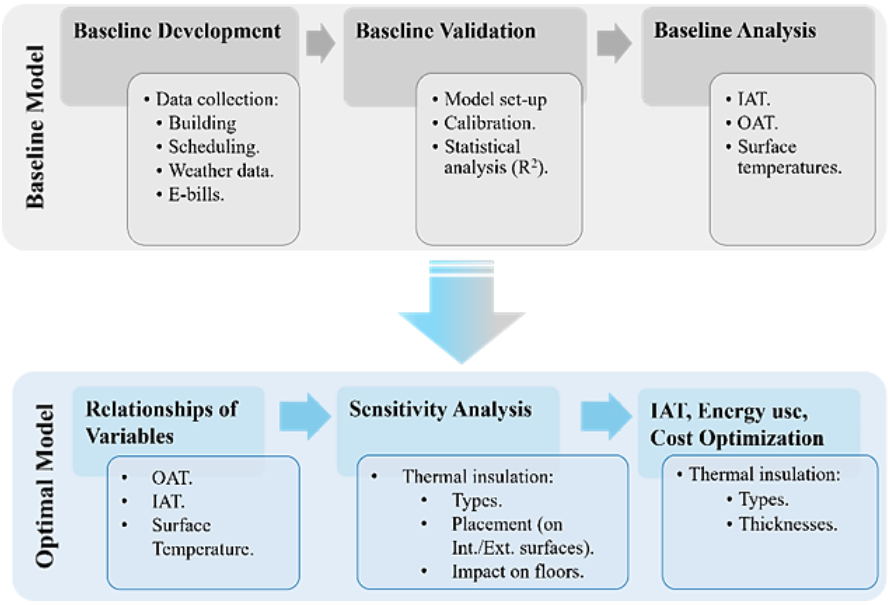

Figure 3. Research methodology

3.1 Building model development

Developing a robust baseline energy model is a critical step in benchmarking and assessing the impact of thermal-insulation retrofitting measures on IAT, energy performance, and operating costs. This process requires comprehensive building data inputs that accurately represent the physical, operational, and environmental characteristics of buildings. By replicating the building's geometry, construction details, systems, and schedules, the model can simulate the energy performance under existing conditions and enable an accurate comparative analysis of various retrofit scenarios.

The input dataset incorporated thermal envelope properties (wall, roof, and floor construction), air infiltration rate, occupancy profiles, lighting and equipment power densities, glazing specifications, window-to-wall ratio (WWR) and dimensional characteristics (floor area, height, and floor count). Additionally, contextual factors, such as the building's geographical location and climatic conditions, were included to ensure that the simulated performance reflected realistic weather conditions. The climatic data for the simulations were sourced from the EnergyPlus Weather files [26] to ensure consistency with established building simulation practices.

The selected case study building was a villa-type residential unit with a total floor area of 525 m². The detailed construction and operational characteristics were adapted from Krarti et al. [14] and are summarised in Table 2. The thermal envelope comprised 20 mm plaster finishes

on both the interior and exterior walls, 150 mm hollow concrete block walls, and a 200 mm reinforced concrete roof slab with 10 mm built-up roofing and 13 mm interior plaster. The floor construction consisted of ceramic tile finishes over a 100 mm concrete slab-on-grade. The windows were single, clear-glazed with wooden frames, representing a common construction approach in the study region, with a WWR of 13 %. The building was operated with an infiltration rate of 0,8 ACH and housed six occupants. The internal loads were defined by a lighting power density of 4,0 W/m², an equipment power density of 3,5 W/m², and a domestic hot water demand of 11,4 L/person/day. Cooling was provided by a split DX system with an energy efficiency ratio of 7,5; operating 24 hours/day with a cooling setpoint of 23 °C.

Table 2. Properties of the villa building energy model [14]

Building model	Villa details
Total floor area	525 m^2
Wall construction	20 mm plaster outside and inside +150 mm concrete hollow block
Roof construction	10 mm built-up roofing + 200 mm concrete roof slab +13 mm plaster inside
Floor construction	Ceramic title + 100 mm concrete slab-on-grade
Glazing	Single-clear with wood frames
Window-to-wall ratio	13%
Air infiltration	0,8 air change per hour
Number of occupants	6
Lighting power density	4,0 W/m^2
Equipment power density	3,5 W/m^2
Domestic hot water	11,4 L/person/day
Cooling set point	23 ^oC
HVAC system	Split DX
Energy efficiency ratio	7,5
Heating/cooling period	24 h/day

To reflect realistic operational conditions, system, lighting, and occupancy schedules were incorporated into the model. These schedules, summarised in Table 3, account for the variations between weekdays (Sunday-Saturday) and weekends (Friday-Saturday). For example, occupancy remained at 100 % during nighttime hours but decreased to 50-70 % during working hours. The lighting and equipment schedules followed similar patterns, with lower usage in the early hours and peaks in the afternoon and evening, consistent with the residential occupancy behaviour in the region.

By integrating these detailed geometric, material, and operational parameters, the baseline model can serve as a reliable reference point for evaluating the performance of alternative insulation strategies. The precision in defining construction assemblies, schedules, and climatic conditions ensured that the subsequent simulation results for both IAT reduction and energy performance were robust, reproducible, and directly applicable to the hot-humid climatic context of the study area.

Table 3. Typical scheduling for the villa baseline energy model [14]

Typical schedule	Hours	Weekdays (Sun-Thu)	Weekends (Fri-Sat)
Occupancy	1-8	100 %	100 %
	8-14	50 %	60 %
	14-22	50 %	70 %
	22-24	80 %	100 %
Lighting	1-8	5 %	---
	8-14	20 %	---
	14-22	60 %	---
	22-24	5 %	---
Equipment	1-8	20 %	20 %
	8-14	30 %	30 %
	14-22	60 %	70 %
	22-24	10 %	10 %

3.2 Model validation

The baseline energy model was rigorously validated to ensure that it accurately represented the actual performance of the reference building and was suitable for the subsequent retrofit analyses. Validation was achieved by comparing the monthly simulated electricity consumption of the model with measured utility data from a comparable villa located in the Riyadh region, as reported by Krarti et al. [14] (see Figure 4). The calibration followed the American Society of Heating, Refrigerating and Air-Conditioning Engineers (ASHRAE) Guideline 14 standards [48, 49], employing iterative adjustments to key parameters, such as internal loads, infiltration rates, and thermostat setpoints, based on real building operational data.

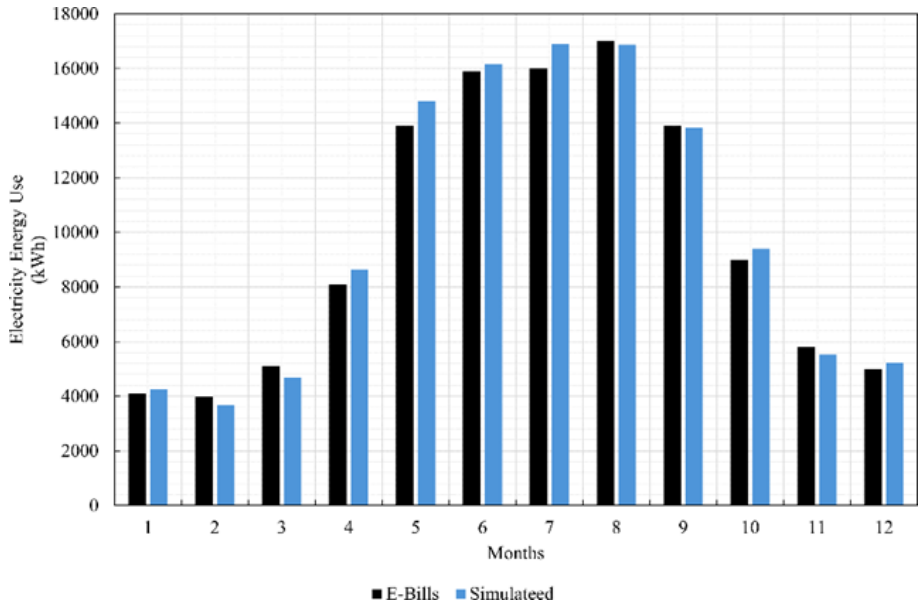

Figure 4. Comparison of the villa's actual electricity bills with the villa's baseline energy model

To enhance accuracy, the model incorporated local hourly weather data, ensuring that the climatic conditions were faithfully represented. The validation results demonstrated a high degree of agreement between the simulation outputs and measured consumption, achieving a coefficient of determination (R^2) of 0,99 well above the ASHRAE recommended threshold of

an R^2 value greater than 0,75 [48; 49]. This strong correlation, presented in Figure 5 and summarised in Table 4, reflects both the stability of the operational profile of the building and the precision of the calibration process.

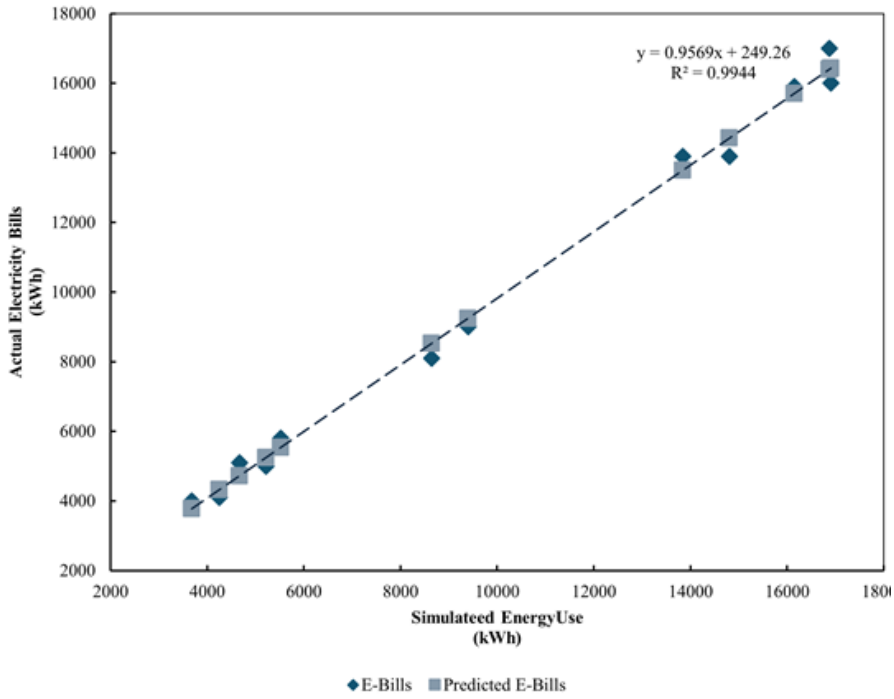

Figure 5. Actual electricity bills and the energy model's electricity use coefficient of performance

Table 4. Descriptive statistics of the energy baseline validation

Descriptive statistics	E-bills (reported data) (kWh)	Simulated (baseline model) (kWh)
Mean	9817	9999
Standard error	1487	1550
Median	8550	9020
Mode	13900	---
Standard deviation	5151	5368
Sample variance	26536061	28819685
Kurtosis	-2	-2
Skewness	0	0
Range	13000	13225
Minimum	4000	3682
Maximum	17000	16907
Sum	117800	119982
Count	12	12
Largest value	17000	16907
Smallest value	4000	3682
Confidence level (95%)	3273	3411

Although discrepancies in building energy modelling often arise from occupant behaviour variability or construction quality differences, such gaps were minimal in this study because of

the high-quality input data, climate-specific calibration, and systematic tuning applied. Consequently, the validated baseline model provided a robust and reliable foundation for evaluating the energy and economic impacts of thermal insulation retrofitting measures in subsequent analyses.

3.3 Sensitivity analysis

SA was conducted to evaluate the influence of thermal insulation type, placement, and thickness on IAT. The objective was to quantify the relative impact of each insulation configuration and establish relationships between the outdoor air temperature (OAT), IAT and surface temperatures. This process enhances the understanding of heat transfer through the building envelope and supports the identification of effective retrofit strategies.

This analysis was performed in two steps. First, the correlation between OAT and IAT was examined to establish the baseline thermal behaviour of the building. Second, the relationship between the OAT and the mean inner and outer surface temperatures of the building envelope was analysed. These relationships offer deeper insights into the thermal interactions between the external and internal environments, thereby enabling targeted optimisation of the building envelope.

Five commonly available thermal insulation materials in the Saudi market board, batt, cellular glass (CG), fibreglass (FG) and polyurethane (poly) were applied to both the interior and exterior surfaces of the baseline envelope. To determine the performance trends, each insulation type was installed individually on the exterior surface, with thicknesses increased in 25 mm increments up to 100 mm. The resulting IAT changes were recorded for each configuration.

The final stage of the analysis extended beyond the IAT evaluation to assess the energy consumption and associated electricity costs for each insulation configuration, thereby linking the thermal performance improvements to their operational and economic implications.

4 Results

This section presents the findings of the study to achieve the research aim: evaluating the impact of various thermal insulation configurations on IAT, energy performance and electricity costs in a hot-humid climate using a validated dynamic simulation model.

4.1 Air temperature assessment

4.1.1 OAT, IAT and surface temperature

To understand the heat transfer of the envelope and its impact on the rising indoor air temperature, the frequencies of OAT and IAT were identified, followed by the surface temperature and the relationship between air temperature and mean internal and external surface temperatures. Figure 6 illustrates that OAT in the Jazan region is predominantly hot, with temperatures consistently exceeding 28 °C for approximately 55 % of the time. IAT analysis of the villa baseline indicated discomfort, surpassing the recommended thermal comfort boundaries set by ASHRAE, defined as within the range of 18-26 °C. Figure 6 shows that most recorded IAT values were in the high range of 31-34 °C, representing approximately 35 % of the year. This high IAT was due to solar radiation that raised the OAT and delivered heat from the outer to the inner environment, emphasising the need for thermal insulation implementation. At baseline, the IAT was uncomfortable for approximately 93 % of the year, accounting for 8151 hours, while only 7 % equivalent to 609 hours was within the comfort range defined by ASHRAE [48; 49]. This necessitates the implementation of various thermal-envelope insulation applications on the inner and outer surfaces of envelopes to assess their sensitivity and determine their optimal placement.

To assess the role of the building envelope in heat transfer and its influence on the increased IAT, the analysis first examined the frequency distribution of the OAT and IAT, followed by an evaluation of the surface temperatures and their relationship with the mean internal and external surface conditions. As shown in Figure 6, the OAT in the Jazan region is

predominantly hot, exceeding 28 °C for approximately 55 % of the year. An analysis of the baseline villa model revealed significant thermal discomfort, with the IAT frequently surpassing the ASHRAE-defined thermal comfort range of 18-26 °C. Notably, the majority of IAT values fell within the high range of 31-34 °C, representing approximately 35 % of annual hours.
This elevated IAT can be primarily attributed to solar radiation gains, which increase the OAT and drive heat transfer through the envelope from the external environment to the internal environment. Consequently, the baseline IAT remained outside the comfort range for approximately 93 % of the year (8 151 hours), with only 7 % (609 hours) falling within ASHRAE's comfort limits of the ASHRAE [48; 49]. These findings highlighted the need for thermal envelope insulation to mitigate heat transfer, improve thermal comfort, reduce energy usage, and lower electrical costs.

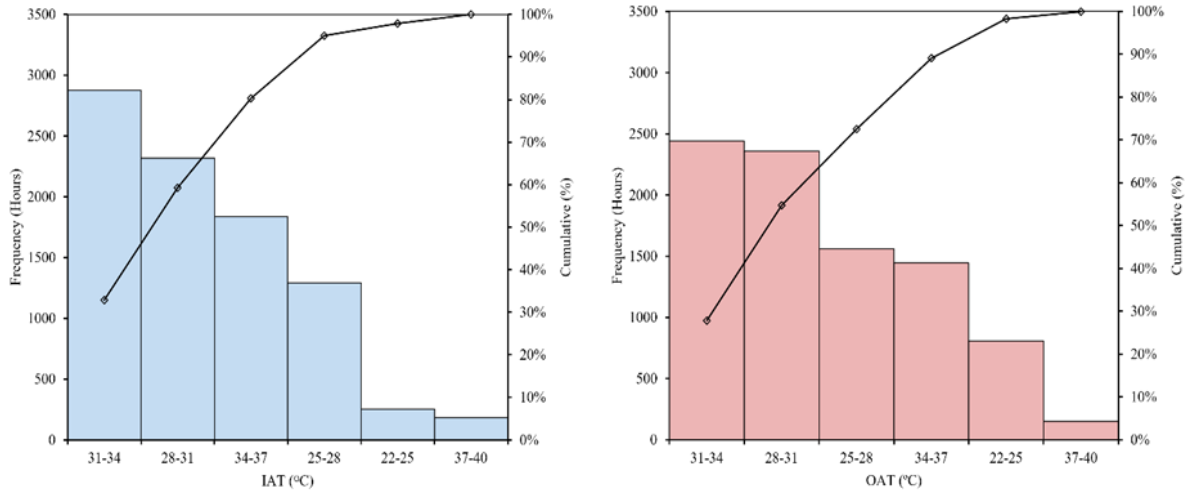

Figure 6. Baseline indoor air temperature (IAT) and outdoor air temperature (OAT) in Jazan

Alosaimi [7] reported that across Saudi Arabia, mean surface temperatures most frequently fall within the 29-35 °C range for approximately 52 % of the year (4500 hours), indicating a strong potential for these conditions to elevate IATs. Building on this, surface temperature patterns were examined specifically in the Jazan region, where the climatic conditions are characterised by persistently high heat and humidity. As shown in Figure 7, the results revealed a clear relationship between OAT, IAT and mean surface temperature. Higher OAT drives higher surface temperatures, in turn increasing IAT. Exterior surfaces absorb heat primarily from solar radiation, and a portion of this energy is transferred through the envelope to the interior surfaces. According to the First Law of Thermodynamics, heat flows from hotter to cooler regions; consequently, elevated interior surface temperatures radiate heat into the indoor environment. This radiative heat gain contributes to heat accumulation, intensifying thermal discomfort, and highlights the critical role of thermal insulation in mitigating envelope heat transfer in Jazan's hot-humid climate.
Compared to Alosaimi's Saudi-wide findings [7], the Jazan-specific results of this study demonstrated an even greater persistence of high surface temperatures, reflecting the region's hot-humid microclimate. This radiative heat gain contributes to significant heat accumulation indoors, intensifying thermal discomfort, and underscoring the critical role of thermal insulation in mitigating envelope heat transfer in the climate of Jazan.

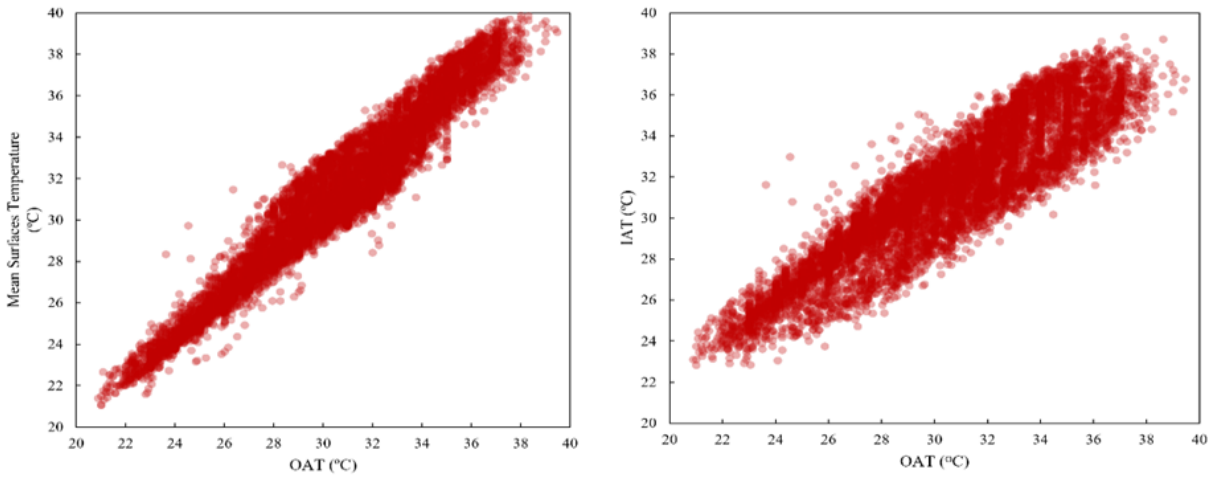

Figure 7. Correlation between outdoor air temperature (OAT), indoor air temperature (IAT) and mean surface temperature

4.1.2 Thermal insulation

IAT assessments are essential for reducing energy consumption while maintaining acceptable thermal comfort conditions. Thermal insulation within a building envelope can be placed on the external or internal surfaces. Previous research in Riyadh demonstrated that external insulation placement is generally more effective [7] because it reduces both envelope heat transfer and air infiltration rates. However, no similar investigations have been conducted on Jazan's hot-humid climate, necessitating SA to determine the optimal insulation placement in this context.

In this study, the five most commonly used insulation materials in the Saudi market—board, bat, CG, FG and poly were selected based on their prevalence in building applications and their distinct thermal characteristics. Their properties, including thermal conductivity, R-value, density, and specific heat capacity, are summarised in Table 5. These parameters were used as direct inputs in the simulation model to ensure that the performance differences could be attributed to material properties under identical environmental and boundary conditions. All insulation layers were modelled using a contact insulation system applied directly to the building envelope without an air cavity to eliminate thermal buffering effects and focus on material-driven performance.

Table 5. Properties of each thermal insulation material

Material	Thermal conductivity (W/m·K)	R-value (m²·K/W)	Density (kg/m³)	Specific heat capacity (J/kg·K)
Board	0,0300	35	100	1400
Batt	0,0475	25	400	1800
CG	0,0450	40	1200	1700
FG	0,0400	30	800	1600
Poly	0,0325	38	35	1900

The analysis initially compared the impacts of interior and exterior insulation placement on IAT. The results shown in Figure 8 indicate that the external insulation placement consistently yielded superior performance, reducing heat transfer through the envelope and lowering infiltration rates, thereby improving the airtightness of the building shell. Based on these findings, subsequent analyses of the insulation type and thickness were conducted exclusively with external placement.

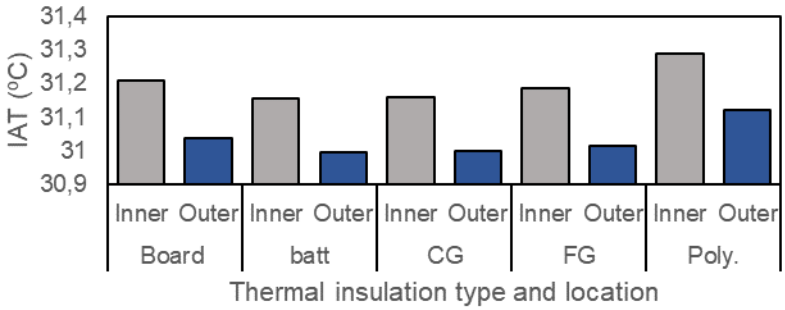

Figure 8. Sensitivity of thermal insulation (Board, Batt, Cellular Glass (CG), Fibre Glass (FG), and polyurethane (Poly)) placement on the thermal envelope

The insulation performance is influenced by multiple factors, including surface exposure to solar radiation, site context, application conditions, local climate, building design, insulation type, and thickness. An additional floor-level SA was conducted to assess the variation in insulation effectiveness between the first and second floors (Figure 9). The results showed that the first floor exhibited a positive linear relationship between insulation thickness and IAT, with increased insulation slightly increasing the indoor temperatures. In contrast, the second floor demonstrated an inverse relationship, with a greater insulation thickness resulting in a lower IAT. This difference can be attributed to the reduced exposure of the first floor to solar gains, the ceiling being shaded by the upper floor, and the smaller surface area in contact with external climatic conditions. In contrast, the second floor showed a strong inverse relationship with increased insulation thickness, leading to a substantial reduction in IAT. This enhanced performance on the second floor can be attributed to its greater exposure to solar gains owing to the direct roof contact and larger proportion of surfaces exposed to the external environment. Consequently, the second floor benefits more from additional insulation, which reduces heat transfer through both the roof and walls, thereby lowering the IAT. Overall, these findings highlight that optimal insulation strategies must account for building-specific characteristics, especially surface exposure and floor-level differences, to maximise thermal performance in hot-humid climates, such as Jazan.

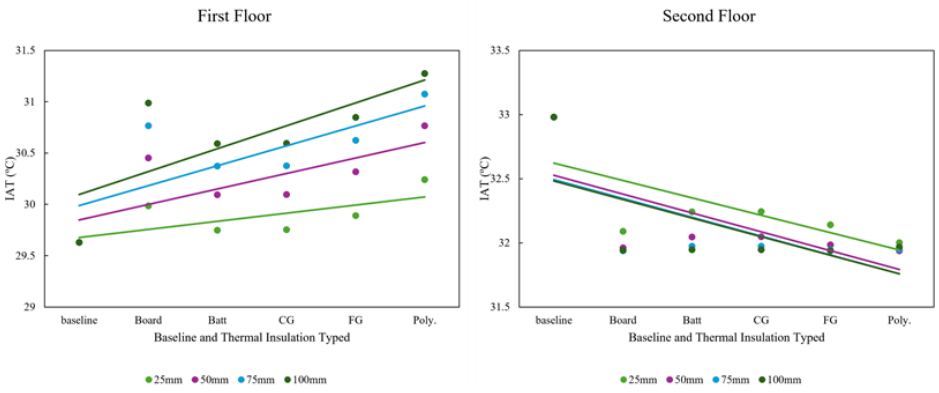

Figure 9. Correlation between floor Indoor Air Temperature (IAT) and thermal insulation types (board, batt, cellular glass (CG), fibreglass (FG), and *polyurethane* (*Poly*))

Overall, the board insulation thicknesses exhibited minimal variations in IAT on the second floor, whereas clear differences were observed on the first floor (Figure 10). The relatively constant IAT values on the upper floor were primarily due to the high solar heat gain through the exposed roof surface. On the first floor, the lowest IAT was achieved with a 25 mm board thickness, indicating that thinner insulation performed better under hot and humid conditions, possibly owing to the reduced thermal resistance, allowing for better moisture dissipation. In

humid climates, excess moisture can reduce the effective performance of thick insulation materials, thereby limiting their benefits.

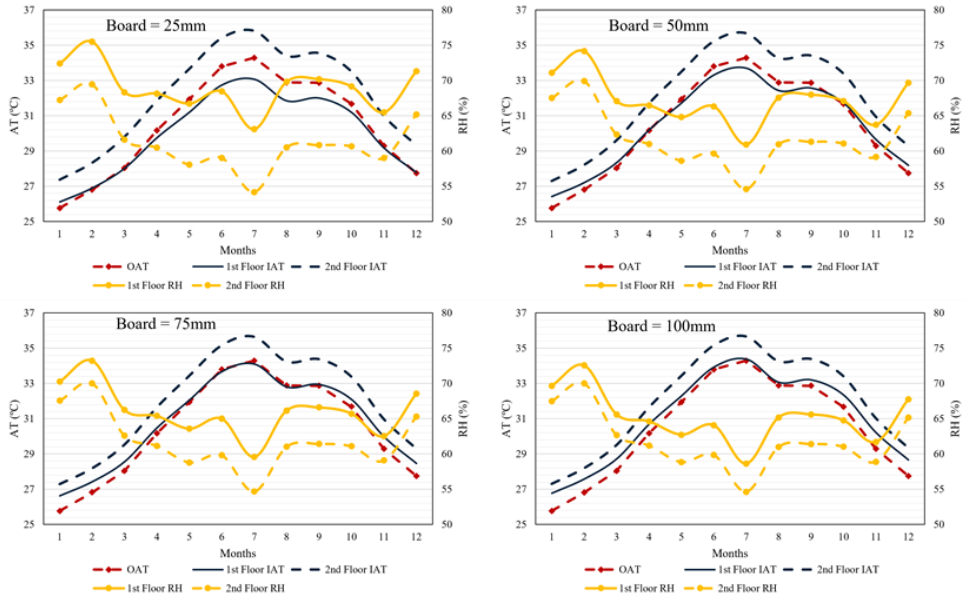

Figure 10. Indoor air temperature (IAT), Outdoor air temperature (OAT), and relative humidity (RH) with board thermal insulation applied on the exterior surface of the baseline

Figure 11 illustrates that the batt insulation on the first floor achieved cooler temperatures with an optimal thickness of 25 mm. Although thicker insulation theoretically offers higher thermal resistance, its marginal gains in humid environments are offset by the moderating effect of moisture on heat transfer. Consequently, the additional costs and materials required for greater thickness may not be justified.

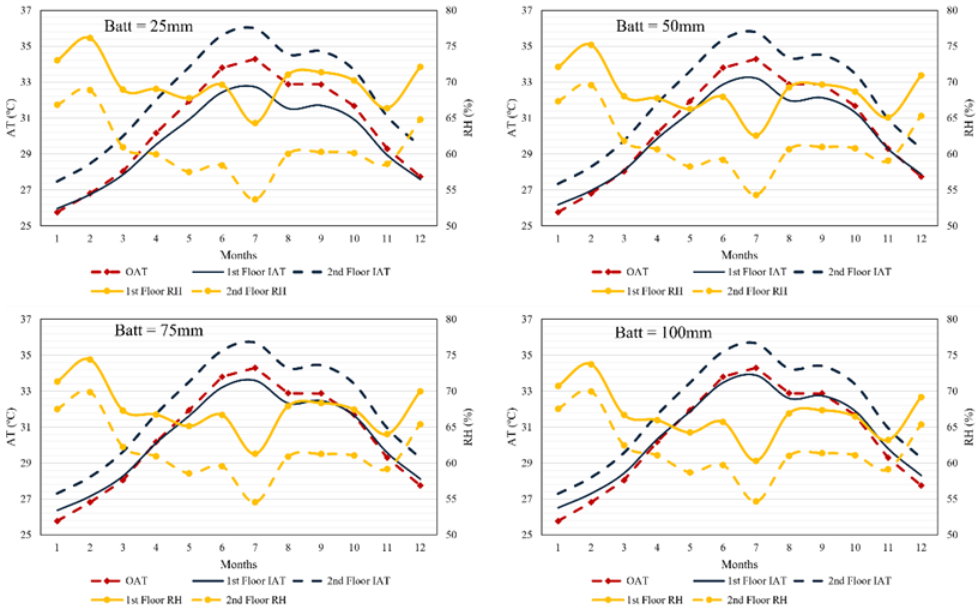

Figure 11. Indoor air temperature (IAT), outdoor air temperature (OAT), and relative humidity (RH) with batt thermal insulation applied on the exterior surface of the baseline

As shown in Figure 12, CG insulation performed optimally at 25 mm on the lower floor but required 100 mm on the upper floor to offset the roof-exposed solar gains. The superior performance of CG at higher thicknesses in roof applications can be attributed to its nonporous, moisture-resistant structure, which maintains its thermal resistance even under humid conditions [50]. FG insulation exhibited similar trends, with a better performance on the first floor, whereas the optimal thickness for the upper floor was 75 mm, which compensated for the heat gain from the roof (see Figure 13). Poly insulation, as shown in Figure 14, performed best with a 25-mm thickness on the first floor and showed comparable behaviour on the upper floor.

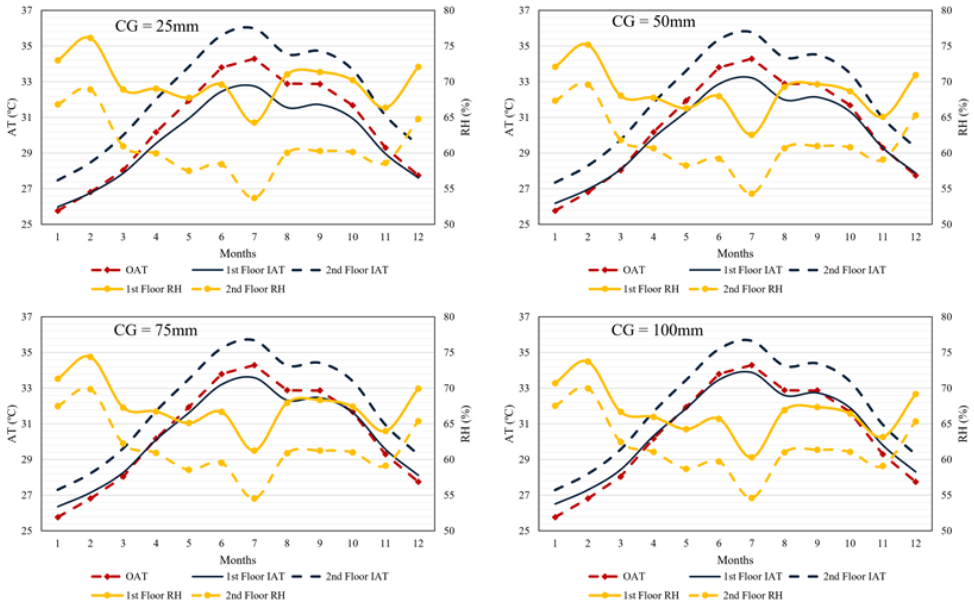

Figure 12. Indoor air temperature (IAT), outdoor air temperature (OAT), and relative humidity (RH) with cellulose glass (CG) thermal insulation applied on the exterior surface of the baseline

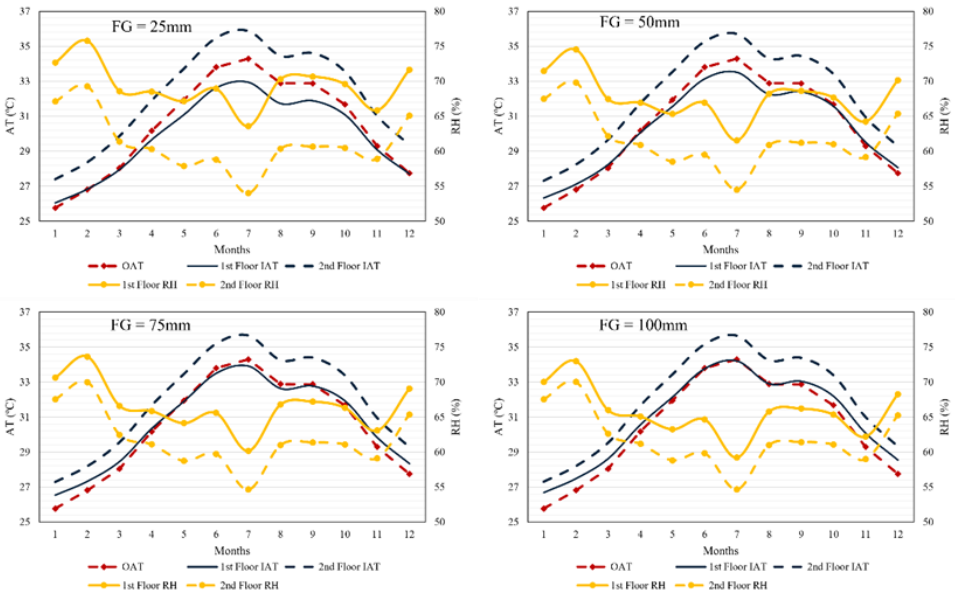

Figure 13. Indoor air temperature (IAT), outdoor air temperature (OAT), and relative humidity (RH) with fibreglass (FG) thermal insulation applied on the exterior surface of the baseline

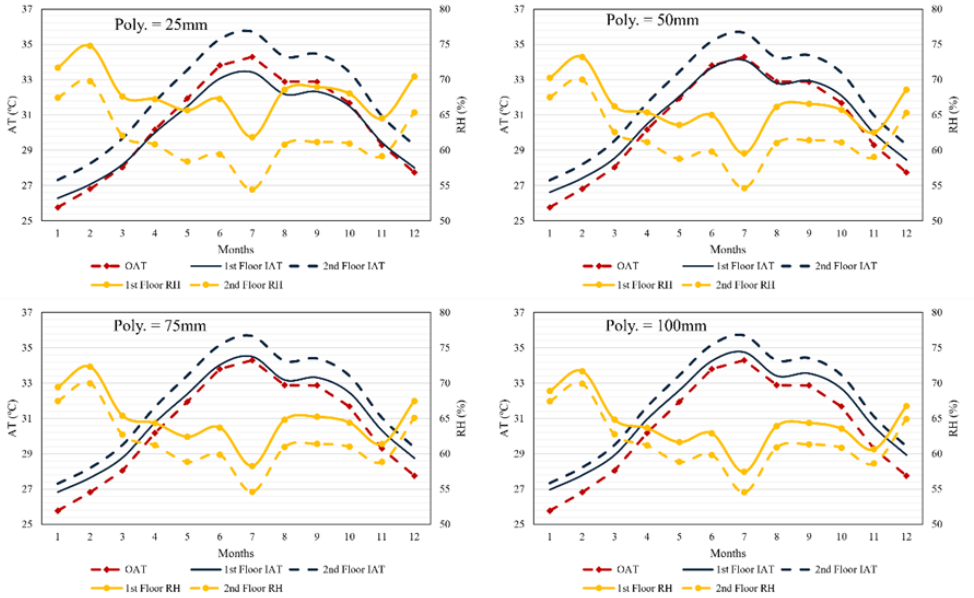

Figure 14. Indoor air temperature (IAT), outdoor air temperature (OAT), and relative humidity (RH) with polyurethane (Poly) thermal insulation applied on the exterior surface of the baseline

These findings diverge from those of Alosaimi [7] in a dry climate, where thicker insulation consistently improved performance. This difference is likely due to the hot-humid conditions of Jazan, where moisture dynamics influence insulation effectiveness. The results suggest that the optimal insulation thickness varies not only by material type, but also by floor level. In general, upper floors with exposed roofs require thicker insulation to counteract high solar heat gains, whereas lower floors benefit from thinner insulation owing to reduced exposure and the mitigating influence of humidity.

The box plot in Figure 15 compares the IAT of the baseline and the five thermal insulation types at the four thicknesses each. The upper and lower bars depict the highest and lowest IAT values, respectively. The central bar represents the median value, and the black box illustrates one standard deviation from the mean, which is represented by the × sign. The lowest data variance was associated with the polythermal insulation type, with a mean IAT of 31,4 ºC and a median of 31,6 ºC. This was followed by the board thermal insulation type, with a mean IAT of 31,2 ºC and a median of 31,4ºC. The lowest mean IAT value was 31,1 ºC, with a median of 31,2 ºC, for batt and CG thermal insulations.

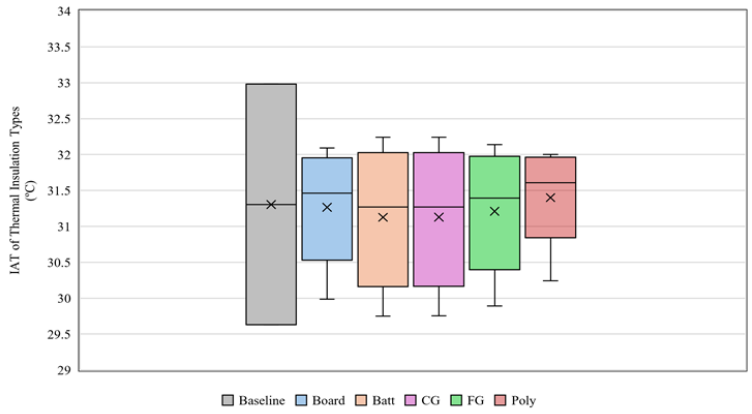

Figure 15. Indoor air temperature (IAT) of the baseline and thermal insulation types (board, batt, cellular glass (CG), fibreglass (FG), and *polyurethane* (*Poly*))

Figure 16 shows the differences between the mean and median values of the five types of thermal insulation. The dashed blue line represents the mean value at baseline, and the black box indicates the difference between the mean and median values. Batt and CG insulation types lowered the IAT the most, both with mean values of 31,12 ºC compared to the baseline's 31,30 ºC IAT. These were followed by FG, board and poly, with mean values of 31,21 ºC, 31,26 ºC and 31,41 ºC, respectively. Figure 17 illustrates the temperature difference (ΔT) in the IAT achieved by each insulation material relative to the baseline uninsulated case. Of the five tested materials, batt and CG yielded the greatest temperature reduction, with ΔT values approaching +0,25 °C, indicating superior thermal performance in lowering indoor temperatures. FG provided a moderate improvement of approximately +0,10 °C, followed by board, which exhibited the least reduction, at just under +0,05 °C. In contrast, poly demonstrated a negative ΔT of –0,10 °C, suggesting that it was the least effective insulation material for reducing IAT under the simulation conditions. Poly performed worse without air conditioning (AC) or insulation because of heat retention. These results highlight the varying thermal behaviours of insulation materials and the importance of context-specific evaluations when selecting insulation types for high-performance building applications.

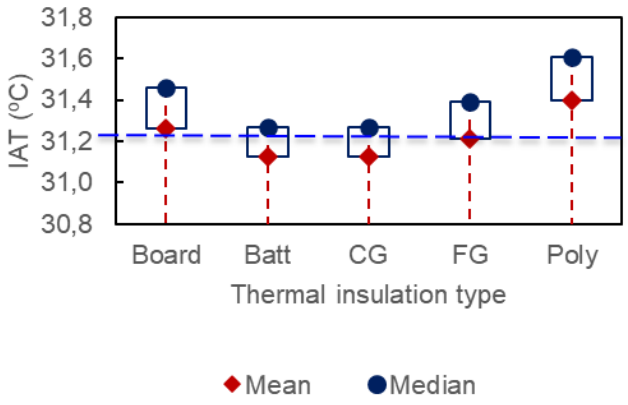

Figure 16. Mean and median indoor air temperature (IAT) values of thermal insulation types (board, batt, cellular glass (CG), fibreglass (FG), and *polyurethane* (*Poly*)) and the baseline (dashed blue line)

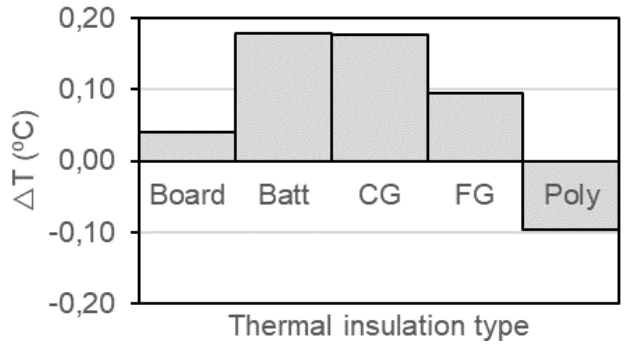

Figure 17. Indoor air temperature (IAT) differences between the baseline and insulation types (board, batt, cellular glass (CG), fibreglass (FG), and *polyurethane* (*Poly*))

4.2 Energy performance comparison

4.2.1 Thermal insulation

Figure 18 presents the monthly energy consumption in kilowatt hours over a 1 year period for the baseline building envelope and multiple insulation configurations. The baseline scenario,

indicated by the red dashed line, represents the baseline without additional insulation upgrades and exhibits the highest energy consumption throughout the year. The annual energy performance revealed significant seasonal variations, with consumption peaking during the summer months (June-August) owing to increased cooling loads, reaching a maximum of approximately 17000 kWh in July. This elevated summer demand reflects the high thermal gains through the building envelope in the absence of adequate insulation.

In contrast, all insulation configurations board, batt, CG, FG and poly at thicknesses ranging from 25 to 100 mm demonstrated considerable reductions in energy consumption compared with the baseline. The degree of reduction is strongly correlated with both the material type and the insulation thickness. Poly with a thickness of 100 mm Poly 1, represented by the blue dashed line consistently achieved the lowest energy use across all months, with the peak summer consumption reduced to approximately 6200 kWh. This represents an approximately 64% reduction compared to the baseline peak, highlighting the superior thermal resistance and air-sealing capabilities of this material. Although Poly achieved the lowest impact on IAT without air conditioning because of its ability to retain heat, it performed better when air conditioning was active because of its superior thermal resistance and airtightness.

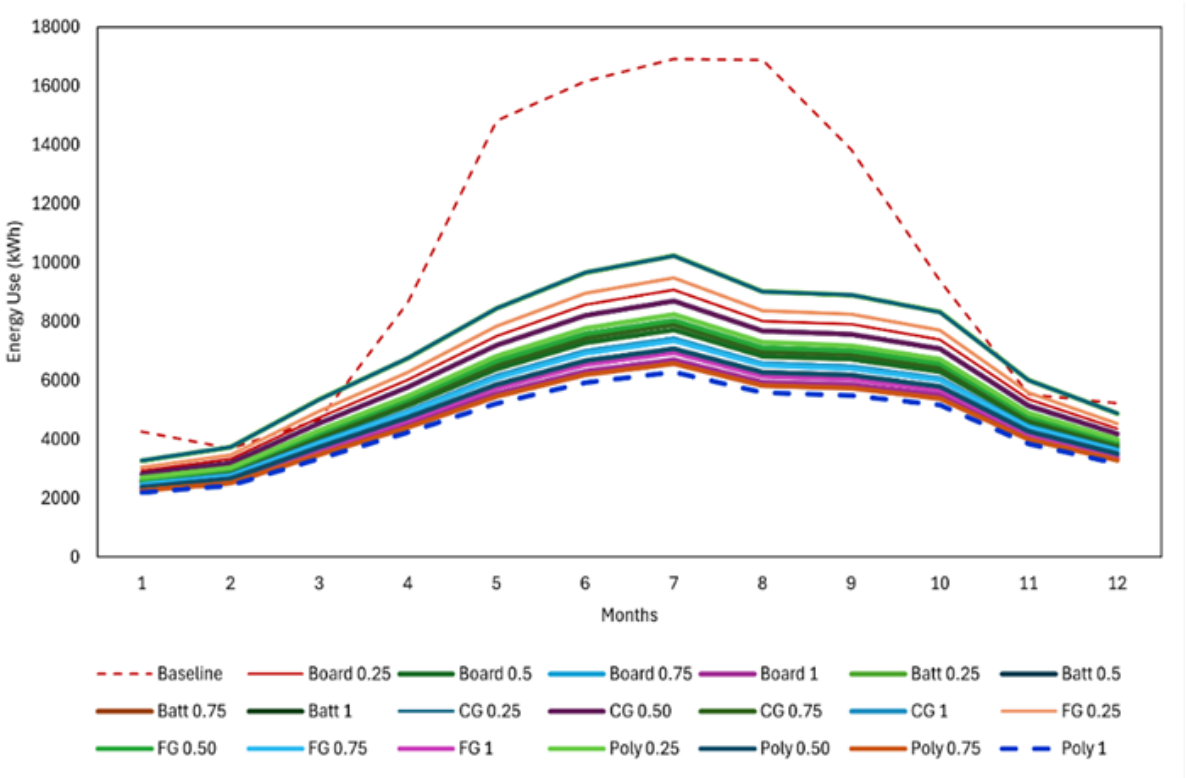

Figure 18. Energy consumption of the baseline compared to the various thermal insulation types and thicknesses (board, batt, cellular glass (CG), fibreglass (FG), and *polyurethane* (*Poly*))

Poly has low thermal conductivity (0,0325 W/m·K) and a high R-value (38 m²·K/W), giving it excellent resistance to conductive heat transfer. Its low density (35 kg/m³) and relatively high specific heat capacity (1900 J/kg·K) make it highly effective at reducing heat gains under active cooling. However, in the free-running mode, these same properties can trap internal heat, leading to a higher IAT compared with materials such as Batt or CG. Batt, with higher density (400 kg/m³) and specific heat capacity (1800 J/kg·K), and CG, with the highest density (1200 kg/m³) and R-value (40 m²·K/W), can absorb and release heat more gradually, offering better passive comfort. FG and board exhibited intermediate properties, resulting in a moderate performance. The differences highlight that low-conductivity materials like Poly perform better

when running the cooling system but may be less favourable in unconditioned scenarios compared to higher-mass insulations.

For all insulation types, increasing the thickness led to further reductions in energy use. For example, for FG, the energy consumption progressively declined from 25 to 100 mm, illustrating the cumulative effect of the additional thermal resistance. Notably, the performance hierarchy across the materials was relatively consistent, with poly outperforming all other materials, followed by FG, CG, batch, and board. These differences can be attributed to variations in thermal conductivity, installation quality, and potential air infiltration control. While insulation primarily reduces conductive heat transfer, certain materials, particularly closed-cell spray Poly, also act as effective air barriers, thereby reducing infiltration rates. Lower infiltration not only decreases the heating and cooling loads but also contributes to more stable indoor conditions.

Seasonal analysis further revealed that the insulation measures yielded the greatest proportional savings during the peak cooling months (May-September), when the thermal gains through the building envelope were the highest. In winter (December-February), although the reductions were less pronounced in percentage terms, they remained significant, reflecting decreased heat loss through insulated walls, roofs, and other envelope components.

Overall, the results clearly demonstrate that both the choice of insulation material and the thickness applied have a substantial impact on building energy performance. High-performance materials such as Poly at greater thicknesses provide the most significant reductions in annual energy use, achieving both conductive heat transfer minimisation and reduced air leakage. These findings highlight the importance of integrating both thermal resistance and airtightness considerations in envelope design to achieve optimal energy efficiency.

Figure 19 illustrates the annual energy use and percentage reductions of various insulation types and thicknesses compared to the baseline, which recorded the highest consumption of approximately 122000 kWh. Among the configurations, Poly at a thickness of 100 mm achieved the greatest energy savings of 40,2 %, followed closely by FG at 100 mm and Poly at 75 mm, both achieving approximately 38,7 % reduction. In contrast, board insulation at 25 mm provided the smallest improvement, with a savings of 24,6 %. These results demonstrate that increasing the insulation thickness generally enhances the performance, although the gains diminish beyond certain levels. Furthermore, materials with lower thermal conductivity, such as Poly and FG, consistently outperform higher-conductivity options. These findings underscore the importance of selecting optimal insulation materials and thicknesses to reduce energy consumption in hot-humid climates such as Jazan.

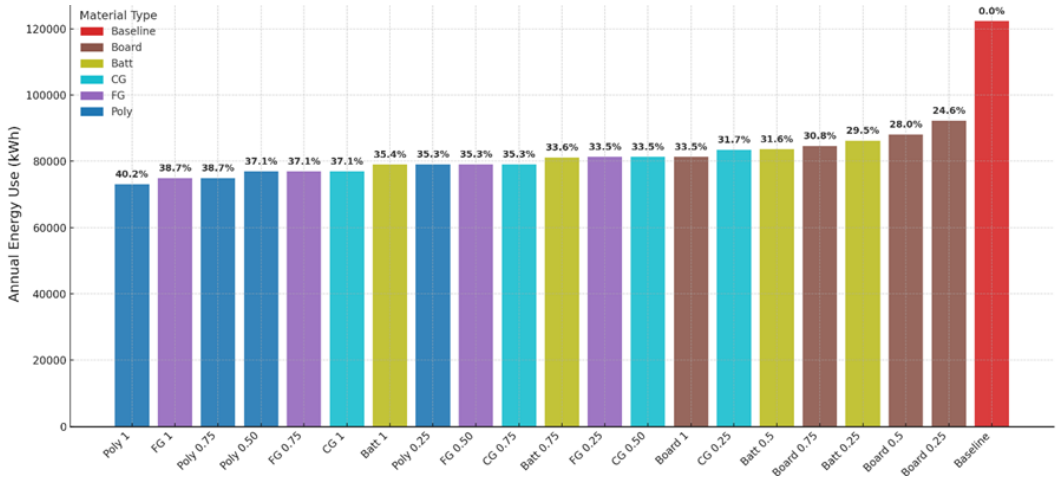

Figure 19. Annual energy use, savings and the percentage of reduction for the insulation types (board, batt, cellular glass (CG), fibreglass (FG), and *polyurethane* (*Poly*)) and the baseline

4.3 Statistical testing

To thoroughly evaluate the significance of the observed energy savings, a series of paired-sample t-tests was conducted to compare the monthly energy consumption for each insulation configuration against the baseline scenario. This method accounts for seasonal variability by pairing the baseline consumption for each month with the corresponding insulation scenario.
Figure 20 indicates that all high-performance insulation configurations achieved statistically significant reductions in energy consumption ($p < 0,05$), confirming that the reductions were not due to random variation but were attributable to the insulation measures. The largest mean monthly difference was observed for poly at 1,0 thickness, which reduced average monthly energy use by approximately 4100 kWh relative to the baseline ($t = 5,53$, $p = 0,000178$). Similar performance was observed for poly (0,75 thickness and FG (1,0 thickness, both yielding mean reductions of approximately 3942 kWh per month ($t = 5,41$, $p = 0,000214$). CG at 1,0 thickness and poly with 0,50 thickness also demonstrated substantial and statistically significant savings, with mean monthly reductions of approximately 3783 kWh ($t = 5,28$, $p = 0,000259$).
These results provide robust statistical evidence that increasing the insulation thickness, particularly with high-performance materials such as closed-cell poly, produces consistent and significant reductions in monthly energy consumption. The low p-values across all the top-performing scenarios reinforce the conclusion that improvements in building thermal performance are both practically meaningful and statistically reliable.

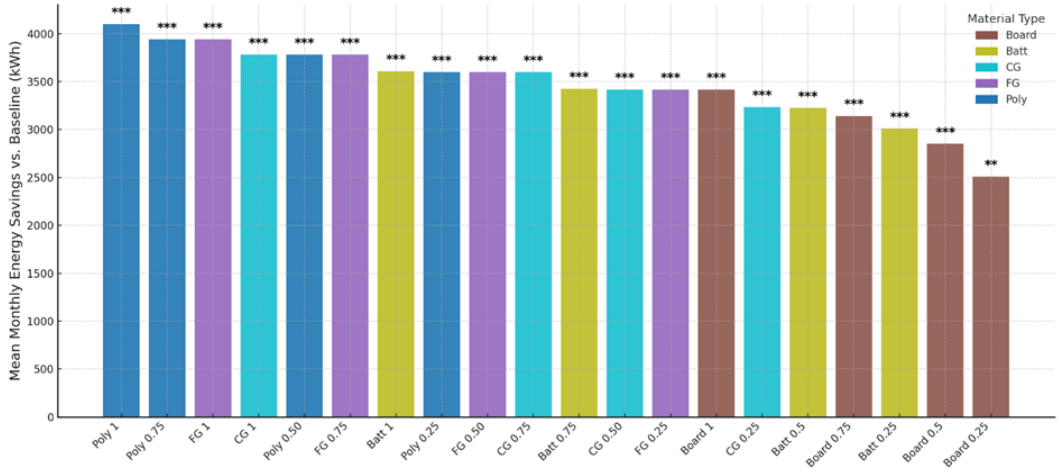

Figure 20. Statistically significant testing of various thermal insulation types and thicknesses (board, batt, cellular glass (CG), fibreglass (FG), and *polyurethane* (*Poly*))

4.4 Cost analysis

Figure 21 presents the comparative annual energy consumption and associated electricity costs of various insulation materials under the Saudi Arabian residential tariff structure. The primary y-axis (left) represents the annual energy use in kilowatt hours, whereas the secondary y-axis (right) displays the corresponding annual electricity cost in USD.
The baseline case with no additional insulation recorded the highest annual energy consumption, of 122300 kWh, resulting in an annual electricity cost of approximately USD 8703. This result reflects the significant cooling and heating loads due to the high heat transfer through the building envelope.
All evaluated insulation types reduced both the energy use and annual cost relative to the baseline. The most substantial savings were achieved by Poly 1, which reduced the annual energy use to 73 100 kWh a 45,82 % cost reduction—corresponding to an annual electricity cost of only USD 4715. Ranked by performance, Poly 1, FG 1 and Poly 0,75 were the top three performers, each delivering major operational savings, while the baseline remained the lowest-performing scenario.

Figure 21 shows the dual-axis format Figure 21. Annual cost comparison between baseline and different types of thermal insulation. This highlights the proportional relationship between the reduced energy consumption and cost savings under the Saudi Arabian tariff. Owing to the tiered pricing structure, reductions in energy use, particularly from high-performance insulation, enable households to avoid the most expensive consumption bands, further amplifying the cost benefits.

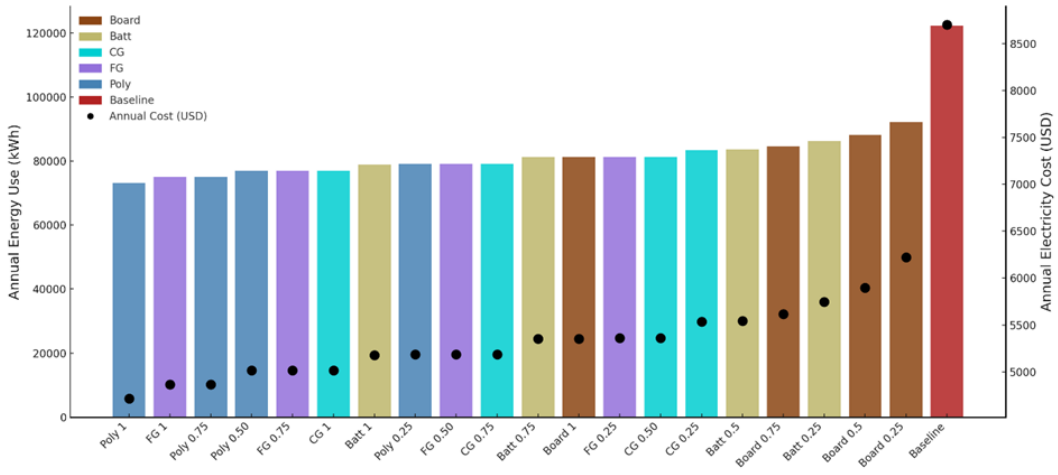

Figure 21. Annual cost comparison between the baseline and types of thermal insulation (board, batt, cellular glass (CG), fibreglass (FG), and *polyurethane* (*Poly*))

4.4.1 Economic implications

Figure 22 presents the projected economic performances of various insulation types in terms of annual, 10-year and 20-year cost savings, along with the percentage savings in annual energy expenditure relative to the baseline. The primary y-axis represents cost savings in USD, whereas the secondary y-axis illustrates the percentage reduction in annual electricity costs.

When projected over a standard building lifespan of 20 years, the annual savings from the best-performing insulation, Poly 1, reached approximately USD 79760 compared with the baseline case (no insulation). Even after accounting for the potential performance degradation over time and moderate increases in electricity tariffs, the cumulative cost reduction remained substantial. These operational savings can offset the initial capital cost of installation within a relatively short payback period, while continuing to provide both financial and environmental benefits for the remainder of the building's service life.

The results show clear differences in performance across the insulation types. High-efficiency materials such as Poly 1, FG 1 and Poly 0,75, delivered the most substantial benefits, with annual cost reductions exceeding 45 % of the baseline. For example, Poly 1 achieved lifetime savings of more than USD 79760 over 20 years under the residential electricity tariff structure in Saudi Arabia. Moderate-performance materials, including Poly 0,5 and FG 0,5, still delivered meaningful savings (25-35 %), rendering them suitable for projects in which initial cost constraints limit material selection.

The annual savings percentage markers plotted on the secondary y-axis highlight a near-linear correlation between insulation thermal performance and cost reduction. This reflects the direct link between reducing the cooling load and lowering electricity consumption. Furthermore, the Saudi tariff's tiered pricing mechanism amplifies these benefits because reducing overall demand helps households avoid higher-cost consumption brackets.

From a long-term financial perspective, investments in high-performance insulation materials yield returns that far exceed the initial outlay, particularly in hot-climate regions with high cooling demands. Even under conservative assumptions, the payback periods for top-

performing materials are estimated to be 3-5 years, after which the building continues to generate net positive cash flows for the remainder of its operational life.

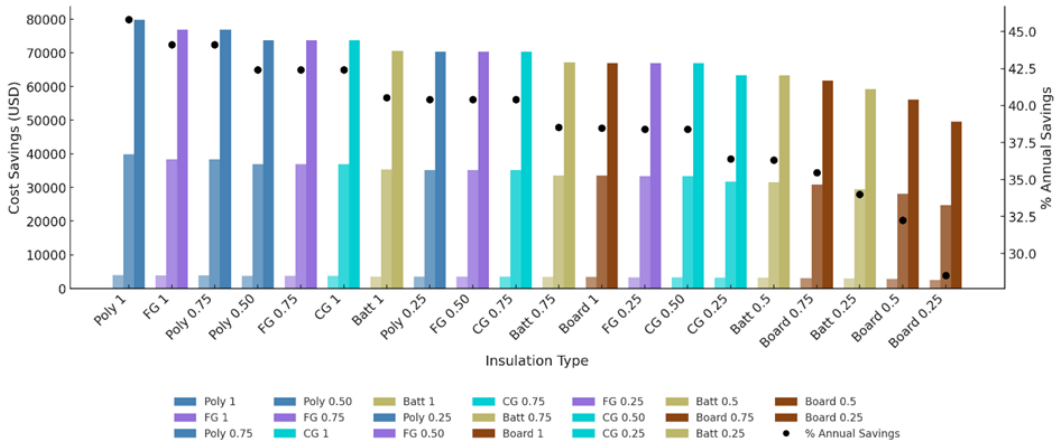

Figure 22. Economic implications of annual, 10-year, and 20-year energy savings when five types of thermal insulation are applied (board, batt, cellular glass (CG), fibreglass (FG), and *polyurethane* (*Poly*))

Figure 23 presents the net present value (NPV) of the projected energy cost savings for various insulation types over a 20-year building lifespan [51], calculated using a 3% discount rate. The NPV, defined as the present value of the cumulative future electricity cost savings relative to a baseline (no insulation), provides a robust measure of the long-term financial return on insulation investment. The bar colours correspond to the specific insulation types.

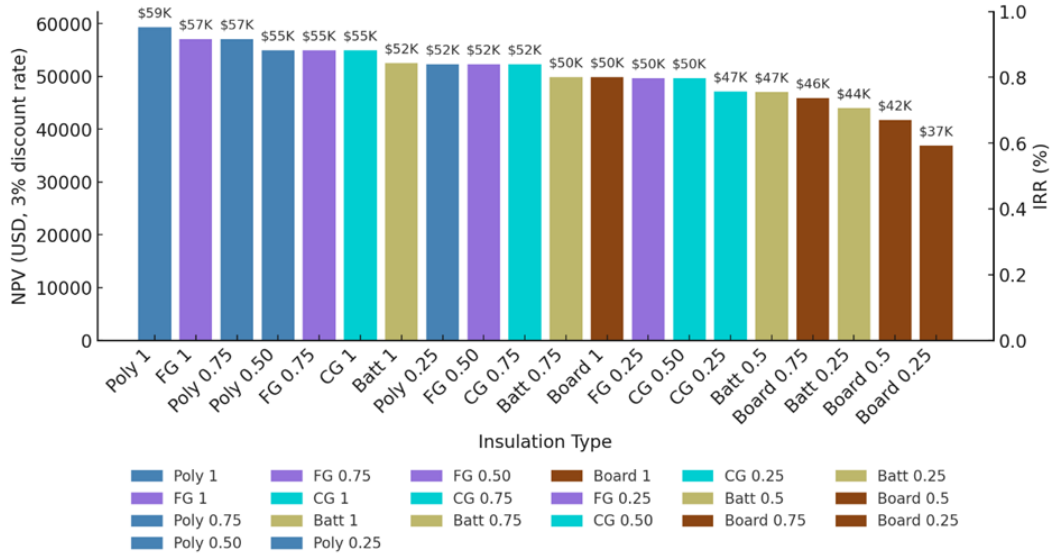

Figure 23. Net present value (NPV) and internal rate of return (IRR) with a 3% discount rate of thermal insulation types (board, batt, cellular glass (CG), fibreglass (FG), and *polyurethane* (*Poly*))

The results indicated significant financial variations across the insulation materials. Poly 1 is the highest-performing configuration, achieving an NPV of approximately USD 59000 over the analysis period, indicating that installing Poly 1 insulation could generate this amount of avoided electricity costs within two decades. FG 1 and Poly 0,75 closely follow, each exceeding NPVs of approximately USD 57000, rendering them strong alternatives for high-performance applications. Mid-range options, such as Poly 0,5 and CG 0,75, deliver NPVs of USD 52000,

representing cost-effective solutions for projects with budget constraints. From an economic perspective, high-performance insulation delivers superior long-term returns, as discounted savings substantially exceed typical initial capital costs. The magnitude of NPV is closely tied to the thermal resistance of the material, with greater reductions in the cooling demand translating into higher lifetime cost savings. Under Saudi Arabia's tiered electricity pricing structure, high-performance insulation provides resilience against tariff escalations by reducing consumption and preventing households from entering higher cost bands.

In addition to NPV, internal rate of return (IRR) values were assessed to evaluate profitability relative to the applied 3 % discount rate, with higher IRR values reflecting more financially attractive options. The abbreviated labels above each bar in Figure 23 (e.g., 59K) show NPVs in thousands of USD for clarity, highlighting that these financial benefits are substantial rather than marginal. Collectively, these results demonstrate that high-grade insulation is a financially sound and environmentally friendly strategy for buildings in hot and humid climates.

5 Limitations and future work

This study was designed to isolate and evaluate the thermal performance of different insulation placements, types and thicknesses under controlled simulation conditions in a hot-humid climate, providing clear insight into their effects on IAT, energy performance and electricity costs. Although this approach enabled robust performance comparisons, it did not account for certain real-world factors, such as construction quality, thermal bridging, material degradation over time, or variations in occupant behaviour and infiltration rates. The analysis was conducted for a single villa typology, which may limit the generalisability across diverse building stocks in Jazan and other hot-humid regions. Furthermore, cost assessment relies on current tariff structures and material prices, which are subject to changes over the lifecycle of a building.

Future research should expand the scope to multiple building types, orientations, and external shadings and include experimental validation under actual operating conditions to verify the simulation results. Integrating life cycle assessment and embodied carbon analysis would enable a more comprehensive sustainability evaluation. Exploring the combined effects of insulation with other passive and active strategies, such as reflective coatings, adaptive shading, advanced glazing, and hybrid ventilation, would provide a fuller understanding of the potential synergies. Scenario modelling that incorporates projected changes in electricity tariffs and climate conditions would further strengthen the applicability of the findings to policymaking and building code development.

Overall, the findings highlighted the dual thermal and economic benefits of optimal insulation strategies in hot-humid climates. They highlighted the importance of tailoring the insulation type and thickness to both material properties and building-specific conditions, including floor level and exposure. Beyond household energy savings, the widespread adoption of optimised insulation practices could contribute to national energy efficiency targets, reduce grid stress during peak cooling demands, and enhance resilience against rising temperatures associated with climate change.

6 Conclusion

The results demonstrated that the insulation placement on the exterior envelope consistently outperformed the interior placement by reducing the conductive heat transfer and infiltration rates. Among the five insulation types assessed—board, batt, CG, FG and poly-poly exhibited the best overall performance owing to their low thermal conductivities and inherent air-sealing properties. Increasing the insulation thickness generally enhanced the performance, although diminishing returns were observed beyond 75-100 mm. The floor-level analysis indicated that upper floors with exposed roofs required thicker insulation to offset high solar gains, whereas lower floors benefitted from thinner insulation, especially under humid conditions where excessive thickness may limit moisture dissipation.

The energy performance analysis revealed annual reductions of up to 40,2 % compared to the baseline, with the most significant savings occurring during the peak cooling months. The economic assessment, based on Saudi Arabia's residential electricity tariff, revealed that high-performance insulation, such as 100 mm poly, could generate lifetime savings exceeding USD 79760 with a net present value (NPV) of approximately USD 5 000 over a 20-year period.
Overall, the findings highlighted the dual thermal and economic benefits of optimal insulation strategies in hot-humid climates. They underscored the importance of tailoring the insulation type and thickness to both the material properties and building-specific conditions, including floor level and exposure. Beyond household energy savings, the widespread adoption of optimised insulation practices could contribute to national energy-efficiency targets, reduce grid stress during peak cooling demands, and enhance resilience against rising temperatures associated with climate change. These findings directly address the identified research gap in the Jazan region by providing region-specific evidence on effective insulation strategies, while also acknowledging that the analysis is limited to modeled scenarios and would benefit from future validation through long-term field studies.

Abbreviations

ACH Air Changes per Hour
BEM Building Energy Modelling
CG Cellular Glass
FG Fiber Glass
GHG Greenhouse Gas
IAT Indoor Air Temperature
IRR Internal Rate of Return
MBPD Barrels per day
ME Middle East
MENA Middle East and North Africa
NVP Net Present Value
OAT Outdoor Air Temperature
Poly Polyurethane
RH Relative Humidity
SA Sensitivity Analysis
TWh Terawatt-hours

References

[1] Our World in Data. Primary energy consumption, 2024. Accessed: July 3, 2024. Available at: https://ourworldindata.org/grapher/primary-energy-cons
[2] Errigo, I. M. et al. Human health and economic costs of air pollution in Utah. Accessed: September 15, 2025. Available at: https://pws.byu.edu/ben-abbott-lab/human-health-and-economic-costs-of-air-pollution-in-utah
[3] U.S. Energy Information Administration. Modeling Distributed Generation in the Buildings Sectors. Accessed June 6, 2024. Available at: https://www.eia.gov/outlooks/aeo/nems/2020/buildings/
[4] Al Ghamdi, A. *Saudi Arabia energy report*. Saudi Arabia: The King Abdullah Petroleum Studies and Research Center (KAPSARC), 2020. https://www.doi.org/10.30573/KS--2020-DP25
[5] World Bank Group. DataBank: Doing Business. Accessed: September 15, 2025. Available at: https://databank.worldbank.org/source/doing-business
[6] Official government website of the Government of the Kingdom of Saudi Arabia. General Authority for Statistics Saudi Arabia. Accessed: September 15, 2025. Available at: https://www.stats.gov.sa/en/
[7] Alosaimi, A. *Optimising the energy performance of the residential stock of the Kingdom of Saudi Arabia by retrofit measures*. [doctoral thesis], University of Nottingham, UK,

2025. Accessed: September 15, 2023. Available at: https://eprints.nottingham.ac.uk/74382/

[8] Rahman, M. M. et al. Energy Demand of the Road Transport Sector of Saudi Arabia—Application of a Causality-Based Machine Learning Model to Ensure Sustainable Environment. *Sustainability*, 2022. 14 (23), 16064. https://doi.org/10.3390/su142316064

[9] Said, S. A. M.; Habib, M. A.; Iqbal, M. O. Database for building energy prediction in Saudi Arabia. *Energy Conversion and Management*, 2003, 44 (1), pp. 191-201. https://doi.org/10.1016/S0196-8904(02)00042-0

[10] Rashidi, S.; Esfahani, J. A.; Karimi, N. Porous materials in building energy technologies—A review of the applications, modelling and experiments. *Renewable and Sustainable Energy Reviews*, 2018, 91, pp. 229-247. https://doi.org/10.1016/j.rser.2018.03.092

[11] Monawar, A. H. *A study of energy conservation in the existing apartment buildings in Makkah Region, Saudi Arabia*. [doctoral thesis], Newcastle University, UK, 2001. Accessed: September 15, 2023. Available at: https://theses.ncl.ac.uk/jspui/handle/10443/950

[12] Aldossary, N. A.; Rezgui, Y.; Kwan, A. Domestic energy consumption patterns in a hot and arid climate: A multiple-case study analysis. *Renewable Energy*, 2014, 62, pp. 369-378. https://doi.org/10.1016/j.renene.2013.07.042

[13] Ates, A. M.; Singh, H. Rooftop solar Photovoltaic (PV) plant – One year measured performance and simulations. *Journal of King Saud University-Science*, 2021, 33 (3), 101361. https://doi.org/10.1016/j.jksus.2021.101361

[14] Krarti, M.; Aldubyan, M.; Williams, E. Residential building stock model for evaluating energy retrofit programs in Saudi Arabia. *Energy*, 2020, 195, 116980. https://doi.org/10.1016/j.energy.2020.116980

[15] Huang, Y.; Dong, C.; Li, D. Research on ventilation cooling devices with low-energy consumption characteristics. *Journal of King Saud University-Science*, 2023, 35 (6), 102759. https://doi.org/10.1016/j.jksus.2023.102759

[16] Delzendeh, E.; Wu, S.; Lee, A.; Zhou, Y. The impact of occupants' behaviours on building energy analysis: A research review. *Renewable and Sustainable Energy Reviews*, 2017, 80, pp. 1061-1071. https://doi.org/10.1016/j.rser.2017.05.264

[17] Swan, L.; Ugursal, I.; Beausoleil-Morrison, I. A *new hybrid end-use energy and emissions model of the Canadian housing stock. In: The 3. Canadian Solar Buildings Conference: the joint 33. annual conference of the Solar Energy Society of Canada Inc. and the 3. Canadian Solar Buildings Research Network conference*. August 20-22, 2008, Fredericton, Canada; 2009.

[18] Kavgic, M. et al. A review of bottom-up building stock models for energy consumption in the residential sector. *Building and Environment*, 2010, 45 (7), pp. 1683-1697. https://doi.org/10.1016/j.buildenv.2010.01.021

[19] Clarke, J. *Energy Simulation in Building Design*. 2nd Edition, UK: Routledge, 2007. https://doi.org/10.4324/9780080505640

[20] Gasparella, A.; Pernigotto, G. Comparison of quasi-steady state and dynamic simulation approaches for the calculation of building energy needs: Thermal losses. In: *International High Performance Buildings Conference*. Purdue University, 2012.

[21] Grandjean, A.; Adnot, J.; Binet, G. A review and an analysis of the residential electric load curve models. *Renewable and Sustainable Energy Reviews*, 2012, 16 (9), pp. 6539-6565. https://doi.org/10.1016/j.rser.2012.08.013

[22] Integrated Environmental Solutions IES. Energy Modelling. Accessed: November 12, 2024. Available at: https://www.iesve.com/services/design-analysis/energy-modelling

[23] U.S. Department of Energy. QuESt 2.0 – Open-source platform for Energy Storage Analytics. Accessed: November 12, 2024. Available at: https://www.sandia.gov/ess/tools-resources/quest

[24] Environmental Design Solutions EDSL. Tas: The complete dynamic building simulation package. Accessed: November 12, 2024. Available at: https://www.edsl.net/tas-engineering
[25] DesignBuilder. DesignBuilder Software. Accessed: November 12, 2024. Available at: https://designbuilder.co.uk
[26] EnergyPlus. EnergyPlus™. Accessed: October 16, 2024. Available at: https://energyplus.net/
[27] Al-Mofeez, I. A. Predicted vs. Actual Energy Savings of Retrofitted House. In: *Proceedings of the Tenth International Conference Enhanced Building Operations*. October 26-28, 2010, Kuwait, Energy Systems Laboratory; 2010, pp. 1-9.
[28] Matar, W. Modeling Residential Electricity Consumption and Efficiency within an Economic Framework: Insights Gained by Using an Engineering-Based Approach. *KAPSARC Discussion Paper*, 2015. https://dx.doi.org/10.2139/ssrn.2675761
[29] Baker, S.; Ponniah, D.; Smith, S. Survey of Risk Management in Major U.K. Companies. *Journal of Professional Issues in Engineering Education and Practice*, 1999, 125 (3), pp. 94-102. https://doi.org/10.1061/(ASCE)1052-3928(1999)125:3(94)
[30] Jones, R. N. Analysing the risk of climate change using an irrigation demand model. *Climate Research*, 2000, 14 (2), pp. 89-100. https://doi.org/10.3354/cr014089
[31] Cullen, A. C.; Frey, H. C. *Probabilistic Techniques in Exposure Assessment: A Handbook for Dealing with Variability and Uncertainty in Models and Inputs*. 1st Edition, USA: Springer, 1999.
[32] Kleijnen, J. P. C. Verification and validation of simulation models. *European Journal of Operational Research*, 1995, 82 (1), pp. 145-162. https://doi.org/10.1016/0377-2217(94)00016-6
[33] Fraedrich, D.; Goldberg, A. A methodological framework for the validation of predictive simulations. *European Journal of Operational Research*, 2000, 124 (1), pp. 55-62. https://doi.org/10.1016/S0377-2217(99)00117-4
[34] Phillips, A.; Janies, D.; Wheeler, W. Multiple Sequence Alignment in Phylogenetic Analysis. *Molecular Phylogenetics and Evolution*, 2000, 16 (3), pp. 317-330. https://doi.org/10.1006/mpev.2000.0785
[35] Ward, M.; Carpenter, T. Simulation modeling of the effect of climatic factors on bluetongue virus infection in Australian cattle herds. I. model formulation, verification and validation. *Preventive Veterinary Medicine*, 1996, 27 (1-2), pp. 1-12. https://doi.org/10.1016/0167-5877(95)00566-8
[36] Limat, S. et al. Cost-effectiveness of CD34+ dose in peripheral blood progenitor cell transplantation for non-Hodgkin's lymphoma patients: a single centre study. *Bone Marrow Transplantation*, 2000, 25 (9), pp. 997-1002. https://doi.org/10.1038/sj.bmt.1702378
[37] Bachrun, A. S.; Ming, T. Z.; Cinthya, A. Building Envelope Component to Control Thermal Indoor Environment in Sustainable Building: A Review. *Sinergi*, 2019, 23 (2), pp. 79-98. http://doi.org/10.22441/sinergi.2019.2.001
[38] Mujeebu, M. A.; Alshamrani, O. S. Prospects of energy conservation and management in buildings–The Saudi Arabian scenario versus global trends. *Renewable and Sustainable Energy Reviews*, 2016, 58, pp. 1647-1663. https://doi.org/10.1016/j.rser.2015.12.327
[39] Al-Naimi, I. M. *The potential for energy conservation in residential buildings in Dammam region, Saudi Arabia*. [doctoral thesis], Newcastle University, UK, 1989. Accessed: September 15, 2025. Available at: https://theses.ncl.ac.uk/jspui/handle/10443/316
[40] Abdelrahman, M. A., Said, S. A. M.; Ahmad, A. A comparison of energy consumption and cost-effectiveness of four masonry materials in Saudi Arabia. *Energy*, 1993, 18 (11), pp. 1181-1186. https://doi.org/10.1016/0360-5442(93)90090-Z
[41] Ahmad, A. Energy simulation for a typical house built with different types of masonry building materials. *Arabian Journal for Science & Engineering*, 2004, 29.

[42] Antar, M. A.; Baig, H. Conjugate conduction-natural convection heat transfer in a hollow building block. *Applied Thermal Engineering*, 2009, 29 (17-18), pp. 3716-3720. https://doi.org/10.1016/j.applthermaleng.2009.04.033

[43] Antar, M. A. Thermal radiation role in conjugate heat transfer across a multiple-cavity building block. *Energy*, 2010, 35 (8), pp. 3508-3516. https://doi.org/10.1016/j.energy.2010.04.055

[44] Budaiwi, I. M. Envelope thermal design for energy savings in mosques in hot-humid climate. *Journal of Building Performance Simulation*, 2011, 4 (1), pp. 49-61. https://doi.org/10.1080/19401491003746639

[45] Al-Sanea, S. A.; Zedan, M.; Al-Hussain, S. Effect of thermal mass on performance of insulated building walls and the concept of energy savings potential. *Applied Energy*, 2012, 89 (1), pp. 430-442. https://doi.org/10.1016/j.apenergy.2011.08.009

[46] Aldawoud, A.; Salameh, T.; Kim, Y. K. Double skin façade: energy performance in the United Arab Emirates. *Energy Sources, Part B: Economics, Planning, and Policy*, 2021, 16 (5), pp. 387-405. https://doi.org/10.1080/15567249.2020.1813845

[47] Alosaimi, A. Evaluating the Sensitivity of Air Infiltration Rates on Envelope Thermal Insulation Performance. *The Saudi Journal of Applied Sciences and Technology*, 2025, 1 (1).

[48] American Society of Heating, Refrigerating and Air Conditioning Engineers ASHRAE. Measurement of Energy, Demand, and Water Savings. Accessed: September 15, 2025. Available at: https://www.ashrae.org

[49] de Dear, R. J.; Brager, G. S. Thermal comfort in naturally ventilated buildings: revisions to ASHRAE Standard 55. *Energy and Buildings*, 2002, 34 (6), pp. 549-561. https://doi.org/10.1016/S0378-7788(02)00005-1

[50] Owens Corning. Foamglass Insulation. Accessed: September 15, 2025. Available at: www.owenscorning.com

[51] Dylewski, R.; Adamczyk, J. Economic and environmental benefits of thermal insulation of building external walls. *Building and Environment*, 2011, 46 (12), pp. 2615-2623. https://doi.org/10.1016/j.buildenv.2011.06.023